MAGNETIC SIMULATION OF AN ELECTROMAGNETIC VARIABLY POLARIZING UNDULATOR*

M. Jaski#, R. Dejus, E. Moog, ANL, Advanced Photon Source, Argonne National Laboratory, Argonne, Illinois 60439, U.S.A.

Abstract

Development of an all-electromagnetic variably polarizing undulator (EMVPU) is underway at the Advanced Photon Source (APS). This device has a set of B_x poles and coils and a set of B_y poles and coils. The B_x coils are powered separately from the B_y coils. Modifying the geometry of the B_x coils or poles changes not only the B_x field but changes the B_y field as well and vice-versa. Magnetic modeling with OPERA 3-D [1] software was used to optimize the coil and pole geometries. Results of the magnetic field simulation and optimization are presented in this paper.

INTRODUCTION

The EMVPU project originated with a request for a device similar to the circular polarizing undulator (CPU) [2] that is installed and in operation at the APS. The EMVPU is a DC magnet with no rapid switching. Electromagnets are used so that the undulator can be operated in several modes: vertical planar, horizontal planar, and right- or left-handed circular or elliptical polarizations. Horizontal and/or vertical quasi-periodicity can also be introduced by reducing the current at the quasi-periodic poles [3]. The original conceptual design of the EMVPU began with very similar geometry as the CPU. Periods as low as 9 cm were evaluated to achieve first harmonic energies as low as 440 eV for vertical polarization and 250 eV for horizontal polarization. It is desirable for the end user to use the shortest possible period length to maximize the flux and brilliance. It is desirable for the magnet engineer to use a longer period length to minimize the magnetic field requirements. The final period length was chosen to be 12.5 cm due to thermal limitations of the coils. Table 1 shows selected design parameters for the EMVPU.

Table 1: EMVPU Selected Design Parameters

PARAMETER	VALUE	UNIT
Period	12.5	cm
Gap	10.5	mm
B_x Effective Field	3308	Gauss
B_y Effective Field	4514	Gauss

THE MAGNET MODELS

Model Geometry

Figure 1 shows the final EMVPU model after optimization. Figure 2 shows the variable dimensions that were used to optimize this model geometry. Table 2 shows the optimal dimensions for this device.

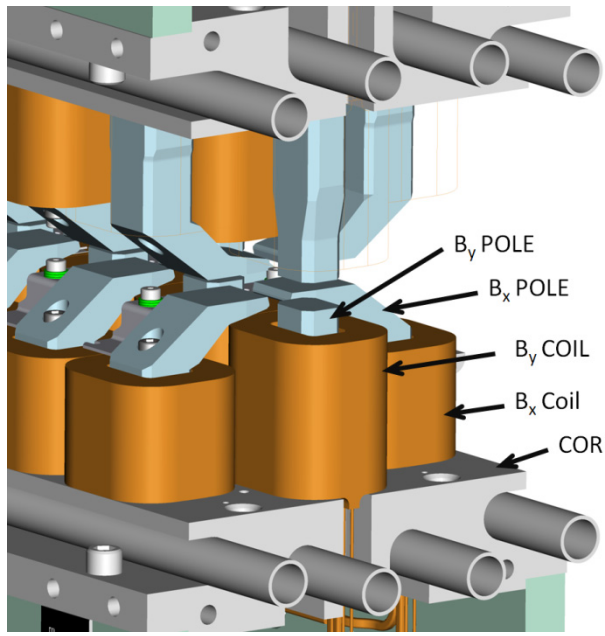

Figure 1: EMVPU model after optimization. The top near three coils are removed to show the top near three poles.

An effort was made to fit the EMVPU to the existing APS long straight section vacuum chamber. This created the 16.25 maximum dimensional restriction shown in Figure 2.

B-H Curves

The pole material is vanadium permendur (VP). VP gives a greater than 12% increase in field compared to poles made out of carbon steel for this device. A prototype was made and the VP B-H curve used for simulations was adjusted to match the measured field. The VP for the prototype was annealed at 820°C. The VP B-H curve in Table 3 gives simulated results that agree with measured results for the geometry of the model presented in this paper to within 1%.

The core material is 1006/1008 steel. Since the flux path area through the core is large, any error in the steel B-H curve will have a negligible effect on the simulated on-axis field. The choice of B-H curve for the steel core is not as critical as the B-H curve for VP.

The Coils

The temperature rise of the coils is one of the dominant restricting obstacles that limits setting the coil currents

*Work supported By U.S. Department of Energy, Office of Science, Office of Basic Energy Sciences, under contract number DE-AC02-06CH11357.

Jaski@aps.anl.gov

Table 2: EMVPU Optimal Dimensions.

I.D.	Description	Optimal Value	unit
A	B_y coil height max	6.3	cm
B	B_x coil height max	5.034	cm
C	B_y pole width	1.823	cm
D*	Conductor size max	0.3264	cm
E*	Conductor size min	0.3231	cm
F	B_x pole gap	1.021	cm
G	B_x pole ball	3.561	cm
H	B_x toenail chamfer	0.404	cm
J	B_x pole toe	0.852	cm
K	B_x tip chamfer z	0.094	cm
L	B_x tip chamfer x	1.176	cm
M	B_x toe tip chamfer x	0.13	cm
N	B_x toe tip chamfer y	0.072	cm
P	B_x cut z	0.131	cm
Q	B_x base height	2.057	cm
R	B_x radius	0.5	cm
S	B_x chamfer	0.276	cm
T	B_x angle	15.5	°
U	B_y tip offset	0.037	cm
V	B_y cut z	0.341	cm
W	B_y base height	5.417	cm
X	B_y radius	0.5	cm
Y	B_y chamfer	0.351	cm
Z	B_y angle	9	°
AA*	Conductor radius	0.081	cm
BB*	Conductor insulation	0.049	cm
CC*	Inner coil fiberglass	0.046	cm
DD*	Outer coil fiberglass	0.036	cm
EE*	Conductor allowance	0.0076	cm
FF	B_x pole height	2.218	cm
GG	B_x pole heel width	2.973	cm

* Not shown in Figure 2

higher to obtain a larger magnetic field. Because of this, limits are set on the power input to each coil, which limits the temperature rise of each coil, which in-turn limits the maximum current to each coil. Thermal analysis (not presented in this paper) establishes that the B_x and B_y coils must be limited to 40 and 45 watts, respectively, for the maximum temperature of the coils not to exceed 100°C. Each time a new magnetic field simulation model is made, the number of turns, conductor length, resistance at 100°C,

Table 3: VP empirical B-H curve

H (Oe)	B (G)
0	0
4.36	7,346
6.43	10,678
8.37	13,045
11.67	15,904
13.82	17,182
21.34	19,642
46.26	20,983
85.82	21,393
188.71	21,586

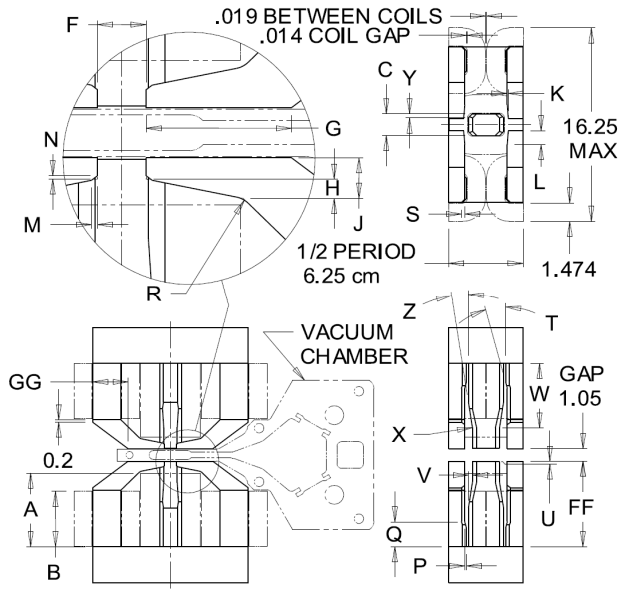

Figure 2: EMVPU geometry.

and maximum currents in each coil are recalculated from the new coil and conductor dimensions.

The resistance calculations are done using the minimum size conductor along with a resistivity at 100°C, giving a conservative heat load estimate. When sizing the coil, the maximum size conductor is used to guarantee the winding array fits within the coil geometry during fabrication.

Both B_x and B_y coils are designed with the same size of square insulated copper conductor. Earlier simulations showed negligible improvement when using different-sized conductors. The coil arrays are determined by fitting as many layers of conductor (maximum size) with insulation, allowances, and fiberglass outer layers as will fit inside the coil cross-sectional dimensions. The inner coil fiberglass dimension is slightly larger to accommodate the Kapton tape used to hold the fiberglass tape in place before epoxy potting. Winding, wrapping, and potting techniques for this coil can be found in [4].

MODELING STRATEGY

Modeling Stages

Magnet simulation models were created in the OPERA 3-D modeler, run in OPERA Tosca, and optimized with the OPERA optimizer software. Analysis was done in several stages. The first stage was to make the smallest possible quick-running analysis model for optimization of a single-period geometry. In the second stage, the mesh was made finer to ensure accurate results with a full-period model. In the third stage, a short four period model was made to properly size the end coils and trim coils and to analyze higher-order integrated multi-pole components (e.g. quadrupole, sextupole, octupole). In the fourth analysis stage, a full-length model was made with quasi-periodic poles. Only stages one and two are discussed in this paper.

Stage One Details

A half-period model with negative-type periodic symmetry is used. The finest part of the mesh is located in the gap, which is the area of interest. Quadratic elements are used in the gap to increase accuracy. Different mesh sizes were tested in order to determine the coarsest possible mesh that would achieve reasonably accurate results. This made optimizing more efficient by allowing the quickest possible run times. Massaging the mesh in this way is necessary because modeling hundreds, if not thousands, of geometric configurations with different geometry and dimensions are required to arrive at the final optimized geometry.

Optimization

The OPERA optimizer allows users to vary as many dimensions as they choose. The dimensions shown in Table 2 were all set as design variables for optimization. Choosing all of the design variables for optimization at the same time results in very long convergence times, however, experience with earlier simulations we found the best choice is to start with optimization of the coil sizes. The pole bases and pole necks can be optimized next while holding the coil sizes constant. Finally, the pole tip geometry can be optimized while holding the coil sizes, pole bases, and pole necks constant. This process is iterated until there is no more improvement in the field.

Each optimization model solved two simulations: one with only the B_x coils energized to full current and one with only the B_y coils energized to full current. The B_x and B_y effective fields were calculated from the B_x and B_y simulations, respectively. The objective is to maximize the sum of the B_x and B_y effective fields while constraining the B_x and B_y effective fields so they are not greater than 3400 and 4600 Gauss, respectively. This will maximize the magnitude of each field that can be obtained without unnecessarily exceeding the required field.

Each time improvements were made to increase the B_x field, the B_y field would decrease. Similarly improving the B_y field would cause the B_x field to decrease. It was a constant battle between B_x and B_y to obtain the best possible solution.

Table 4: Values obtained from stage two optimization

			Circular	
Description	B_x	B_y	B_x	B_y
Current (A)	50.3	47.5	34.2	20.6
Effective Field (G)	3362	4599	2343	2355
Peak Field (G)	3767	5456	2609	2767

Stage Two Details

The final result obtained from stage one optimization is then modeled as a full period with a finer mesh. Table 4 lists the values obtained from stage two optimization.

Figure 3(a) shows a plot for one period of the normalized B_x field as a function of z with only the B_x current turned on. The skew sextupole (BS_3) and skew ten-pole (BS_5) normalized to the B_x peak field are also plotted. The skew sextupole component indicates the maximum B_x field roll-off at x=±3 mm and roll-up at y=±3 mm is about 11%.

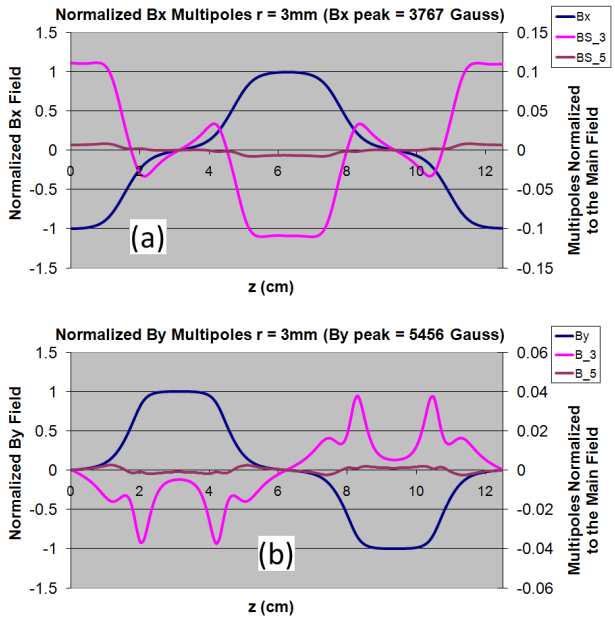

Figure 3: (a) B_x field with skew multi-poles normalized to B_x peak field. (b) B_y field with normal multi-poles normalized to B_y peak field.

Figure 3(b) shows a plot of one period with the normalized B_y field as a function of z for only the B_y current turned on. The sextupole (B_3) and ten-pole (B_5) normalized to the B_y peak field are also plotted. The sextupole component indicates the maximum B_y field roll-off at x=±3 mm and roll-up at y=±3 mm is less than 4%. Similar curves can be obtained for the circular mode.

CONCLUSION

The results presented here provide the optimal shape of the poles and coils for the EMVPU. The methods for solving this problem have been presented. Further simulations that are required include end-pole sizing, trim-coil sizing, multi-pole analysis, and residual-field approximation.

REFERENCES

[1] Opera 3D finite element code, Cobham Technical Services, Oxfordshire, England.
[2] E. Gluskin et al., AIP Conf. Proc. 521, 344 (2000)
[3] R.J. Dejus et al., "Coil Energizing Patterns for an Electromagnetic Polarizing Undulator," these proceedings.
[4] M. Jaski, "Design and Fabrication of Magnet Coils," Diamond Light Source Proceedings, Volume 1, Issue MEDSI-6, p. e7, November 2010.